THE JOURNAL OF BIOLOGICAL CHEMISTRY VOL. 284, NO. 8, pp. 5240–5249, February 20, 2009

Self-assembly of Bacteriophage-associated Hyaluronate Lyase (HYLP2) into an Enzymatically Active Fibrillar Film*

Received for publication, August 29, 2008 Published, JBC Papers in Press, October 10, 2008, DOI 10.1074/jbc.M806730200

Parul Mishra[1] **and Vinod Bhakuni**[2]

From the Division of Molecular and Structural Biology, Central Drug Research Institute, Lucknow 226001, India

The *in vitro* assembly of a soluble protein into its mature fibrillar form is usually accompanied by loss of its functional activity. Our study is the first demonstration of a natural enzyme (HylP2) retaining its enzymatic activity on conversion from prefibril to mature fibril and supports the contention that minor conformational changes in the native folded form of a protein can lead to the formation of a functional fibril. Hyaluronate lyase (HylP2) is a natural enzyme of bacteriophage 10403 of *Streptococcus pyogenes*. At pH 5.0, the enzyme undergoes partial unfolding localized in its N-terminal domain while the C-terminal domain maintains its folded trimeric conformation. This structural variant of HylP2 retains about 70% enzymatic activity with hyaluronan. It further self-assembles into a fibrillar film *in vitro* through solvent-exposed nonpolar surfaces and intermolecular β-sheet formation by the β-strands in the protein. Interestingly, the mature fibrillar film of HylP2 also retains about 60 and 20% enzymatic activity for hyaluronic acid and chondroitin sulfate, respectively. The possession of broad substrate specificity by the fibrillar form of HylP2 indicates that fluctuations in pH, which do not lead to loss of functionality of HylP2, might assist in bacterial pathogenesis. The formation of fibrillar film-like structure has been observed for the first time among the hyaluronidase enzymes. After acquiring this film-like structure in bacteriophage, HylP2 still retains its enzymatic activity, which establishes that these fibrils are a genuinely acquired protein fold/structure.

The phenomenon of transformation of proteins into fibrils is of interest because extracellular fibrillar protein deposits or amyloid plaques are characteristics of a group of neurodegenerative diseases such as Alzheimer disease and Parkinson disease, as well as many rare systemic diseases such as familial amyloid polyneuropathy (1). Despite a lack of identifiable common features in the sequences and structures of the proteins implicated in the different amyloid diseases, the fibrillar aggregates associated with them are characterized by a high degree of structural order and a high intermolecular β-sheet content (2, 3). It has therefore been postulated that there is a common underlying mechanism of formation of the various fibrillar aggregates (4).

It is widely recognized that fibril formation in globular proteins generally requires the presence of a partially unfolded state, referred to as the "amyloidogenic intermediate" (5–8). This can be a conformational state stable at equilibrium, arising as a result of mutations or changes of solution conditions (pH or ionic strength etc.), a partially folded state accumulating transiently before the major free-energy barrier for folding, or one or more conformations resulting from structural fluctuations within the native-state ensemble (9, 10). The requirement of a partially unfolded state is because of the fact that the conformational rearrangements leading to the cross-β-structure cannot take place in a packed folded conformation; a somewhat unfolded conformational state, in which some of the amide and carbon groups and hydrophobic moieties become accessible, can easily enable the specific intermolecular interactions that are necessary for amyloid aggregation to occur (6, 9, 11).

Numerous reports on the loss of biological activity of proteins on the formation of proto-fibrils from native protein forms and fibrils from proto-fibrillar forms have been stated (12, 13). Fibrillation in nonpathological proteins leads to loss of their biological function, whereas pathological proteins acquire toxicity in proto-fibrillar forms (14–16). To date, the presence of enzymatic activity in mature fibrils of any protein has not been reported. However, functionally active amyloid-like fibrils of a designed RNase A have recently been reported (17). In addition to being present in the microorganisms, there is a naturally occurring functional amyloid in mammals (Pmel17) that functions as a template for the polymerization of melanin molecules in the melanosome (18), and thus strengthens the view that fibrillar structures could rather be a selected protein fold in the evolution of functional protein structures. These contradictory findings then raised the need to address an important question pertaining to fibrillar structure that whether native-like structural domains undergo conformational modification or they simply refold on fibril formation.

The *hylP2* gene of bacteriophage 10403 of *Streptococcus pyogenes* encodes an enzyme hyaluronate lyase (HylP2)[3] whose primary function is to degrade hyaluronan of the bacterial capsule (19). We carried out biophysical characterization (20) and x-ray data analysis of HylP2 (Protein Data Bank code 2DP5), which demonstrated that the C-terminal domain of the protein predominantly consisted of β-sheets harboring the active site residues (20). To date there is no report on the presence of amyloid-like fibrillar structures in the bacteriophage of *S. pyogenes*,

* The costs of publication of this article were defrayed in part by the payment of page charges. This article must therefore be hereby marked "*advertisement*" in accordance with 18 U.S.C. Section 1734 solely to indicate this fact.
[1] Supported by the Council of Scientific and Industrial Research, New Delhi, India.
[2] To whom correspondence should be addressed: Division of Molecular and Structural Biology, Central Drug Research Institute, Lucknow 226001, India. Fax: 91-522-223405; E-mail: bhakuniv@rediffmail.com.

[3] The abbreviations used are: HylP2, hyaluronate lyase; ThT, thioflavin T; CR, Congo red; ANS, 1-anilino-8-*N*-naphthalenesulfonic acid; HA, hyaluronic acid; CS, chondroitin sulfate.

although the bacterium itself has been reported to possess amyloid-like M proteins on its surface, which help in spreading bacterial infection by facilitating the attachment of this Gram-positive bacterium to host soft tissues (21).

Our work, for the first time, highlights the transformation of a functional, natively folded and nonfibrillar natural enzyme (HylP2) into fibril- like structures that appear as a thin membrane. This form of protein is different in morphology from the disease-causing fibrils known to date, and the presence of enzymatic activity in such structures provides indications toward their plausible role in the biology of the organism. In bacteriophage, these structures can be considered to assist in phage access into the bacterial cells even under stress conditions (altered pH).

EXPERIMENTAL PROCEDURES

Materials

Escherichia coli DH5α cells were used during the cloning of the gene. pET21d(+) vector (Novagen) and BL21 (DE3) cells (Novagen) were used for protein expression.

Methods

Cloning, Overexpression, and Purification of Full-length HylP2—The cloning, overexpression, and purification of full-length HylP2 was performed as described earlier (20).

Fibril Formation in HylP2—A stock (1 mM) solution of ThT (thioflavin T) was prepared by dissolving ThT in double distilled water. ThT was stored at 4 °C and protected from sunlight. Fresh solutions of ThT were passed through a 0.2-μm filter immediately before use. HylP2 at a concentration of 1 mg/ml was dialyzed in buffer containing 10 mM citrate glycine/HEPES (CGH), 150 mM Na_2SO_4 (sodium sulfate), and 10% glycerol at different pH values. The dialysis was carried out at 4 °C for 14 h. Aliquots were taken at desired time intervals for conducting the pH-related experiments.

Size-exclusion Chromatography—Gel filtration experiments were carried out on a Superdex 200 HR 10/300 column (manufacturer's exclusion limit 600 kDa) with AKTA fast performance liquid chromatography (Amersham Biosciences). The column was equilibrated and run with 10 mM CGH, 150 mM sodium sulfate, and 10% glycerol (at desired pH values). 200 μl (containing at least 0.2 mg protein) of the sample was loaded on the column and run at 25 °C at a flow rate of 0.3 ml/min, and eluted protein was detected at 280 nm.

Fluorescence Measurements—Fluorescence spectra were recorded with a PerkinElmer Life Sciences LS 50B spectrofluorometer in a 5-mm path length quartz cell at 25 °C. For tryptophan fluorescence, excitation wavelength of 290 nm was used, and the spectra were recorded between 300 and 400 nm using 1 μM of HylP2 for the studies. For ANS binding studies, excitation wavelength was 350 nm, and the emission spectra were recorded between 400 and 500 nm. The final concentration of ANS used for the experiments was 10 μM. 5 μM aliquots of the dialyzing samples were added to a solution containing ANS in the dialyzing buffer at pH 5.0 and mixed for 2 min before measuring the fluorescence emission. Background absorption of the buffer for the native HylP2 was subtracted from each reading. All the readings were taken in triplicate.

CD Measurements—CD measurements were made with a Jasco J810 spectropolarimeter. The results were expressed as mean residual ellipticity [θ], which is defined as $[\theta] = 100 \times \theta_{obs}/(lc)$, where θ_{obs} is the observed ellipticity in degree; c is the concentration in moles of residue/liter; and l is the length of the light path in centimeter. Each spectrum was an average of two scans. The values obtained were normalized by subtracting the base line recorded for the buffer under similar conditions. Spectra were recorded using 3 μM HylP2 in 1-mm cell, with 1 mM CGH, 150 mM sodium sulfate, 10% glycerol, at different pH values. All scans were made in the far UV region, *i.e.* between 200 and 250 nm.

Activity Assay—The *in vitro* activity assay for HylP2 was performed using hyaluronic acid (HA) and chondroitin sulfate (CS) as substrates. The activity of the enzyme was determined by measuring its ability to breakdown HA or CS to unsaturated disaccharide units (22). In 1 ml of solution having 0.3 mg/ml HA/CS (or mentioned otherwise), 50 mM sodium acetate buffer, 20 mM calcium chloride (pH 6.0), and 2 μg of full-length native HylP2 at pH 7.0 or the fibrillar form of HylP2 at pH 5.0 (diluted just before taking measurement) was added. The reactants were properly mixed immediately, and the measurements were carried out by monitoring the increase in absorbance at 232 nm for 200 s at 37 °C. Varying concentrations of HA and CS, between 0.003 and 0.3 mg/ml, were used for kinetic measurements. The kinetic parameters were calculated using extinction coefficient of 5.5×10^{-3} M^{-1} for the disaccharide products. The readings were taken in triplicate, and percentage error was calculated.

Transmission Electron Microscopy—HylP2 at a concentration of 1 mg/ml at pH 7.0 and pH 5.0 was diluted 20 times in CGH buffer of pH 7.0 and pH 5.0, placed onto carbon-coated grids, and allowed to adsorb for 4 min. After 5 min, the excess liquid at the edge of the grid was removed with the help of filter paper. The grid was negatively stained with 1% uranyl acetate at pH 7.0 and 5.0 (as required) and air-dried after removing the excess stain. After incubating the grid with dye for 5 min, excess of solution was removed with the help of a filter paper, and the grid was left to dry at room temperature. The grid was then stored in an electron microscope grid box prior to examination. The specimens were viewed, and images were recorded at 80 or 120 kV with an FEI Technai Twin transmission electron microscope equipped with a mega view II CCD camera. Image acquisition and analysis were carried out with analysis software. Low magnification (×10,000–12,000) was used to get an idea of the overall sample composition, and a higher magnification (×25,000) was also used to obtain the sheet-like morphology.

Fluorescence Microscopy—For fluorescence imaging, a Zeiss Axiovert 200 M microscope equipped with an α-Plan-Fluar 100′/1.45 numerical aperture oil immersion objective was used with FluoArc (Zeiss) as light source. Images were captured on 1.4-mega-pixel Zeiss CCD camera AxioCam HRm. Images were acquired and processed using software Axiovision AxioVs40 version 4.4.0.0. For TIRF imaging, TIRF slider coupled with argon ion laser (Lasos, Lasertechnik GmbH, Jena, Germany). 10 μl of HylP2 at pH 7.0 and pH 5.0 at 0.6–1 mg/ml was taken and stained with 2 μl of thioflavin T. The sample was placed on a glass slide, and the image was recorded.

ThT Assay for Determining Kinetics of Fibrillation—Free ThT has excitation and emission maxima at 350 and 450 nm, respectively. However, upon binding to fibrils the excitation and emission λ_{max} changed to 450 and 480 nm, respectively (23). 5 μM aliquots of the HylP2 at pH 7.0 and dialyzed samples of full-length HylP2 at pH 5.0 were added to a solution containing 10 μM ThT in the dialyzing buffer at pH 5.0 and pH 7.0, respectively, and shaken for 5 min before measuring the fluorescence emission on a PerkinElmer Life Sciences LS 50B spectrofluorometer in a 5-mm path length quartz cell at 25 °C. A background fluorescence spectrum obtained by running a blank buffer with ThT was subtracted from each sample fluorescence spectrum. The excitation wavelength was 450 nm, and the emission was recorded at 480 nm. Fluorescence intensity at 480 nm was plotted against time for analysis. All readings were taken in triplicate, and the error bar between them was calculated.

Congo Red Binding—Fresh solutions of Congo red (CR) in 10 mM CGH, 150 mM sodium sulfate (pH 7.0) were passed through a 0.2-μm filter immediately before use. The CR solutions were added to 5 μM of protein solutions (dialyzed at pH 5.0) to a final dye concentration of 10 μM, and the samples were incubated for 2 min. The absorption spectrum of each sample was recorded from 400 to 700 nm on a PerkinElmer Life Sciences UV-visible spectrophotometer using 1-cm path length quartz cuvette and corrected for contributions of buffer and protein. The spectrum of CR alone was compared with that of CR solutions in the presence of protein. Prior to addition of protein, the dye absorbed at 490 nm, and after binding to fibrillar structures a red shift of the absorption band toward 540 nm was observed (24). Red shift together with an increase in absorption was taken to be indicative of the formation of fibrillar structures. Readings were recorded in duplicate protein samples.

Fibril Purification—After dialyzing the native protein into CGH buffer (pH 5.0), the sample was ultracentrifuged at 80,000 rpm for 2 h in a Beckman Coulter Optima TL-X ultracentrifuging system using a TLA 100 rotor. The supernatant was subsequently removed, and the fibril pellet was resuspended in minimal CGH buffer.

Limited Proteolysis—HylP2 protein at pH 7.0 and HylP2 fibrillar film at pH 5.0 were subjected to limited proteolysis with α-chymotrypsin in protease to protein ratio of 1:500 (w/w), for 2 h, at 30 °C. The protease reaction was stopped by adding protease inhibitor EDTA/phenylmethylsulfonyl fluoride to a final concentration of 2 mM in the reaction mixture, and the samples were analyzed on 12% SDS-PAGE. For proteolysis of HylP2 at pH 7.0 and fibrillar film at pH 5.0, proteinase K was used at protein to protease ratio of 100:1 (w/w) for 8–10 h at 30 °C. The reaction was stopped by adding phenylmethylsulfonyl fluoride, and the proteolyzed samples were analyzed on 12% SDS-PAGE.

RESULTS AND DISCUSSION

HylP2 is an ~110-kDa homotrimeric, α/β protein (20) that is devoid of disulfide bonds in its native folded state in the physiological medium. The first few residues from the N-terminal region of HylP2 are an α/β cap-like segment that is followed by α-helical coiled coils to residue 108. This flexible domain proceeds into a highly β-rich C-terminal portion of the protein consisting of 13 parallel β-sheets arranged perpendicular to the axis of the protein (Fig. 1*A*). The last few residues at the C terminus again taper as α-helical coils that do not interdigitate as helical coils of the N-terminal portion of HylP2.[4]

pH-induced Modification in Structural Properties of HylP

pH and salts influence the electrostatic interactions in natively folded proteins and thereby significantly affect the structure, stability, and function of proteins (25). With the aim to probe pH-induced alterations on HylP2, we subjected the protein to pH changes. pH-dependent changes in secondary and tertiary structures of HylP2 were studied using far-UV-CD and tryptophan fluorescence spectroscopy, respectively, and the results are summarized in Fig. 2*A*. The far-UV-CD spectrum shows a negative band centered around 218 nm suggesting the existence of an extended β-sheet conformation in HylP2 at pH 7.0. The intensity of the negative ellipticity band remains steady in pH range from 7.0 to 10.0 suggesting that there is no significant alteration in the secondary structure of the enzyme. However, a slight change (maximum of 15%) in the secondary structure of the enzyme was observed below pH 7.0, suggesting that the secondary structure of HylP2 is significantly resistant to fluctuations in pH.

The changes in tertiary structure of HylP2 as a function of pH were studied, and the results are presented in the Fig. 2*B*. Because HylP2 had a single tryptophan residue at the 19th position in its primary amino acid sequence, which corresponded to the N-terminal region of HylP2 (Fig. 1*A*), any change in the fluorescence emission maximum of this tryptophan residue could be correlated only with the folding or unfolding of the N-terminal region of HylP2. Under physiological conditions (pH 7.0), this tryptophan moiety is buried in the hydrophobic environment as the N-terminal region of the enzyme is in folded conformation (20). The intrinsic fluorescence spectra of the protein showed no significant differences for the wavelength of maximum emission (λ_{max} = 330 nm), whereas on decreasing the pH from 7.0 to 4.0, a noticeable sigmoidal enhancement from 328 to 340 nm in the emission wavelength was observed. The buried tryptophan residues in all folded proteins show fluorescence emission maxima between 330 and 335 nm, whereas proteins in unfolded conformation show fluorescence emission maxima at about 350 nm (26). The red shift of the λ_{max} value from 328 to 340 nm at acidic pH conditions suggested that under these conditions the tryptophan moiety present in the enzyme was partially exposed to the hydrophilic solvent because of partial unfolding of the N-terminal domain. The studies presented above suggested that with fluctuations in pH (pH <6.0), HylP2 probably undergoes a single conformational transition where the native-like protein was converted into a quasi-native state having a slightly disorganized N-terminal domain and a native-like C-terminal domain architecture of protein.

To confirm the existence of partially unfolded species with solvent-exposed hydrophobic clusters, we performed pH-dependent ANS binding studies on HylP2. ANS is a hydrophobic dye that binds to solvent-exposed hydrophobic surfaces of a

[4] P. Mishra, V. Bhakuni, R. Prem Kumar, N. Singh, S. Sharma, P. Kaur, and T. P. Singh, unpublished data.

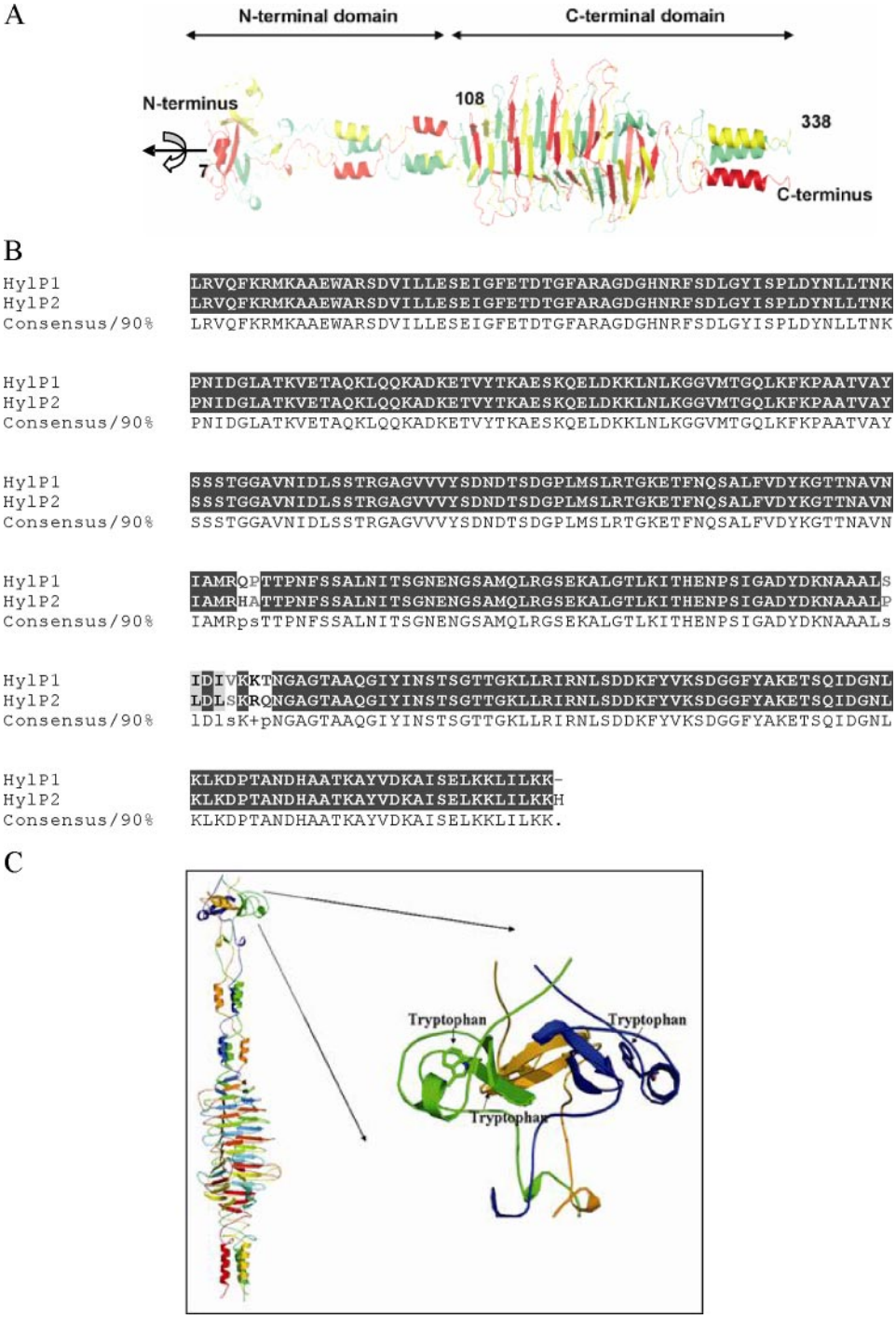

FIGURE 1. **The three-dimensional structure of HylP2.** *A,* complete molecular stereo view showing the intertwining polypeptide chains colored in *yellow, red,* and *green* that represent its homotrimeric configuration. The distinct domain topology can be seen with the N-terminal domain showing an α-helical coiled segment extending from residue 1 to 108 and the β-rich groove of C-terminal from residue 121 to 297. The structure has been generated using PyMOL. The x-ray crystal structure of HylP2 has been submitted by P. Mishra, V. Bhakuni, R. Prem Kumar, N. Singh, S. Sharma, P. Kaur, and T. P. Singh (Protein Data Bank code 2DP5). This protein bears >90% identity to HylP1 (Protein Data Bank code 2C3F). The structural details related to 2C3F have been published by Smith *et al.* (44). *B,* ClustalW of HylP2 with HylP1. *C,* zoomed image of the N-terminal region of HylP2 showing the tryptophan residue at position 19th in all the three chains of HylP2. The image is created using PyMOL.

polypeptide chain. In a native folded protein the hydrophobic amino acids were buried in the core of the protein, and ANS binding is not observed; hence, the emission wavelength maximum of free dye is observed to be at 514 nm (Fig. 2*B, inset*). However, on partial unfolding of the protein, ANS shows binding to the solvent-exposed hydrophobic amino acids, which led to a shift in the fluorescence emission maximum of the dye to 465 nm accompanied by an enhancement in the fluorescence intensity (27–29). We monitored the affinity of protein for ANS binding at 465 nm as a function of pH. As observed in Fig. 2*B*, between pH 10.0 and 6.0, the increase in the fluorescence emission intensity of ANS was negligible. However, on decreasing the pH from 6.0 to 4.0, a large enhancement (about four times) in the ANS fluorescence intensity was observed. This suggested that although the hydrophobic regions of the enzyme remained encompassed in the core of HylP2 in the alkaline and physiological pH range, thereby not allowing the ANS molecules to bind to them, acidic conditions caused the exposure of hydrophobic patches in the enzyme because of the unfolding of the protein. Hence, the tryptophan and ANS fluorescence studies together reaffirmed that subjecting the protein to acidic conditions led to the stabilization of a partially folded intermediate of HylP2.

Modifications in the quaternary structure were also monitored under pH conditions that were stabilizing the partially unfolded species of HylP2. Size-exclusion chromatography studies were then carried out at different pH values, and the results are shown in Fig. 2*C*. HylP2 at pH 7.0 had a retention volume of 13.07 ml, which corresponded to a molecular mass of about 110 kDa, which corresponded to the trimeric conformation of the protein. However, on decreasing the pH to 5.0 and below, a retention volume of 8.30 ml was observed that corresponded to the void volume of the gel filtration column and a molecular mass of about 600 kDa or more for the protein. This suggested that under acidic conditions, HylP2 underwent significant enhancement in its hydrodynamic radii probably because of aggregation of the enzyme. This was finally confirmed by glutaraldehyde cross-linking. At pH 5.0, the cross-linked protein sample did not even enter the well in SDS-PAGE (Fig. 2*D*), which suggested that the cross-linked protein

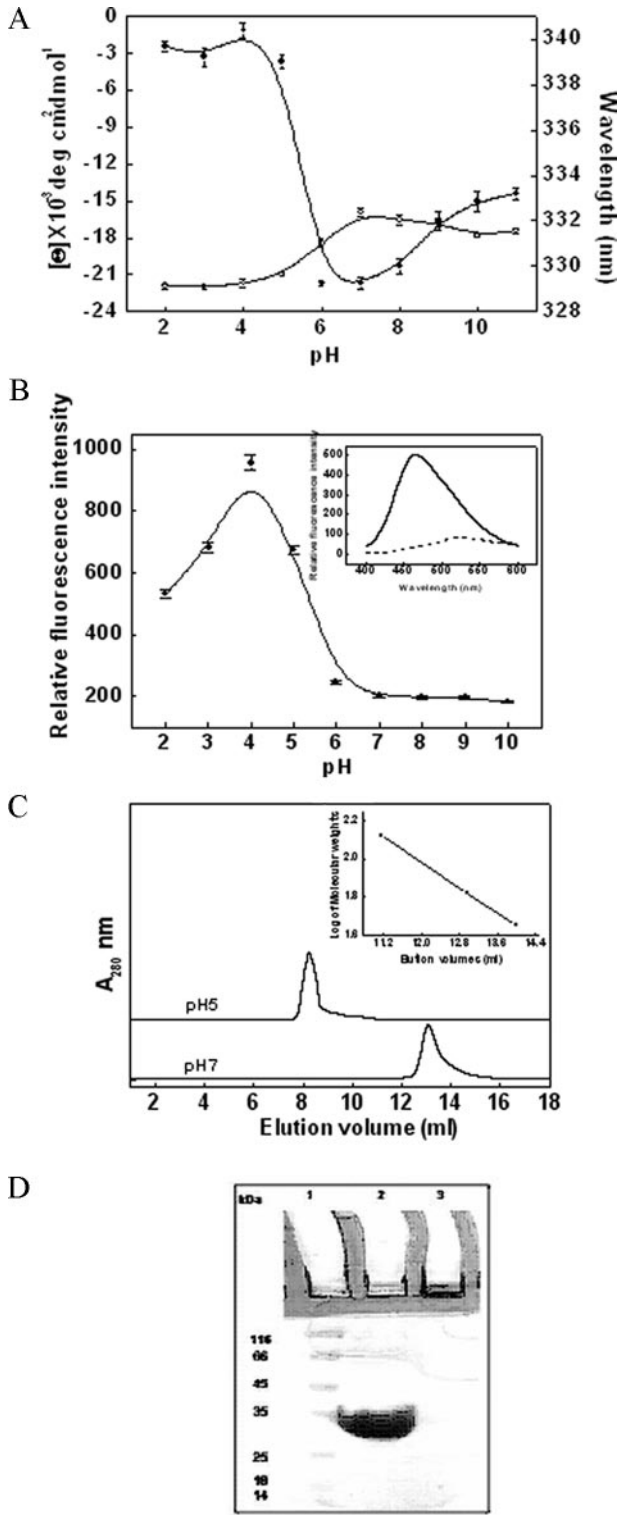

FIGURE 2. **Structural changes in HylP2 at 25 °C as a function of pH.** *A,* changes in ellipticity at 218 nm (○) and tryptophan fluorescence emission wavelength (●) of recombinant HylP2 with change in pH. *B,* pH-dependent changes in ANS fluorescence intensity on binding to HylP2. *Inset* shows the changes in the ANS fluorescence spectra at of HylP2 at pH 5.0 (*solid line*) and pH 7.0 (*dashed line*). *C,* size-exclusion chromatographic profiles for HylP2 on Superdex 200 HR column at pH 7.0 and pH 5.0 at 25 °C. The column was calibrated with standard molecular weight markers, glucose oxidase (160 kDa), albumin (66 kDa), ovalbumin (43 kDa), and ribonuclease (13.7 kDa). *D,* 10% SDS-PAGE profile of glutaraldehyde cross-linked form of HylP2 at pH 5.0. *Lane 1* represents molecular weight markers; *lanes 2* and *3* represent uncross-linked native HylP2 and glutaraldehyde cross-linked form of HylP2 at pH 5.0, respectively.

had a very large molecular weight that was possible only when the protein was aggregated under these conditions.

Overall the analysis presented here indicated that HylP2 populated under aggregating conditions (pH 5.0) had a partially unfolded N-terminal domain and a folded C-terminal domain indistinguishable from the native protein, and with time these protein molecules coalesced into a HylP2 aggregate form.

Characterization of Aggregates of HylP2 Formed under Acidic Conditions

Dye Binding—To assess the existence of fibrous texture in the aggregates of HylP2 formed at low pH (pH 5.0 and below), their tinctorial and ultrastructural properties were examined. The aggregates of HylP2 were characterized by monitoring its binding to thioflavin T and Congo red dyes and then morphologically analyzed by transmission electron microscopy.

Congo red, a diazo dye, is widely used to identify fibrils because it binds preferentially to the ordered, aggregated form of peptides/proteins but does not bind to their native unassembled forms (24, 30). We carried out Congo red binding to HylP2 to identify the existence of fibril-like features in the aggregates of HylP2 stabilized at pH 5.0. Fig. 3*A* shows the effect of binding of Congo red (to HylP2 dialyzed at pH 7.0 and 5.0) on the absorption spectra of the dye. Binding of Congo red to proteins is detected as a red shift in its absorbance spectrum from 490 to 520 nm. For the enzyme at pH 7.0, no shift in the absorption maximum and absorption intensity of the dye was observed. However, on incubation of the enzyme at pH 5.0 with Congo red, a red shift of about 20 nm in the absorption maxima, *i.e.* from 490 to 510 nm, of the dye was observed. Such a prominent red shift in the absorption maxima was attributed to the strong intercalation of the dye into the ordered, intermolecular β-pleated sheet structure of the HylP2 fibrils. Hence, this indicated that the aggregates of HylP2 formed at pH 5.0 had fibril-like characteristics. An increase in the absorption intensity at 510 nm of HylP2 at pH 5.0 suggested a decrease in the native form of the protein and an increase in the population of fibrillar species, respectively.

ThT is a fluorescent dye and is known to bind to the linear array of β-strands in the amyloid fibrils. An enhancement in the fluorescence emission intensity of ThT on binding to ordered aggregates of protein is one of the most accepted methods to show the presence of fibril formation (23, 31) under a given condition. Fig. 3*B* shows the changes in emission intensity of ThT at 480 nm on binding to HylP2 at pH 7.0 and 5.0. For enzyme at pH 7.0, the fluorescence intensity was similar to that shown for ThT alone suggesting that the dye does not bind to native HylP2. However, for the enzyme at pH 5.0, an emission spectrum having significantly high fluorescence intensity (about 20 times) centered at about 480 nm was observed. This demonstrated that ThT binds to the HylP2 aggregates formed at pH 5.0, which reaffirmed that these aggregates possessed fibril-like properties. Thus, the results of both dye binding assays confirmed that HylP2 forms amyloid-like fibrils at pH 5.0.

Microscopic Assessment of Aggregate Morphology—The morphological features of HylP2 as fibrils at pH 5.0 were unambiguously confirmed by electron microscopy and fluorescence

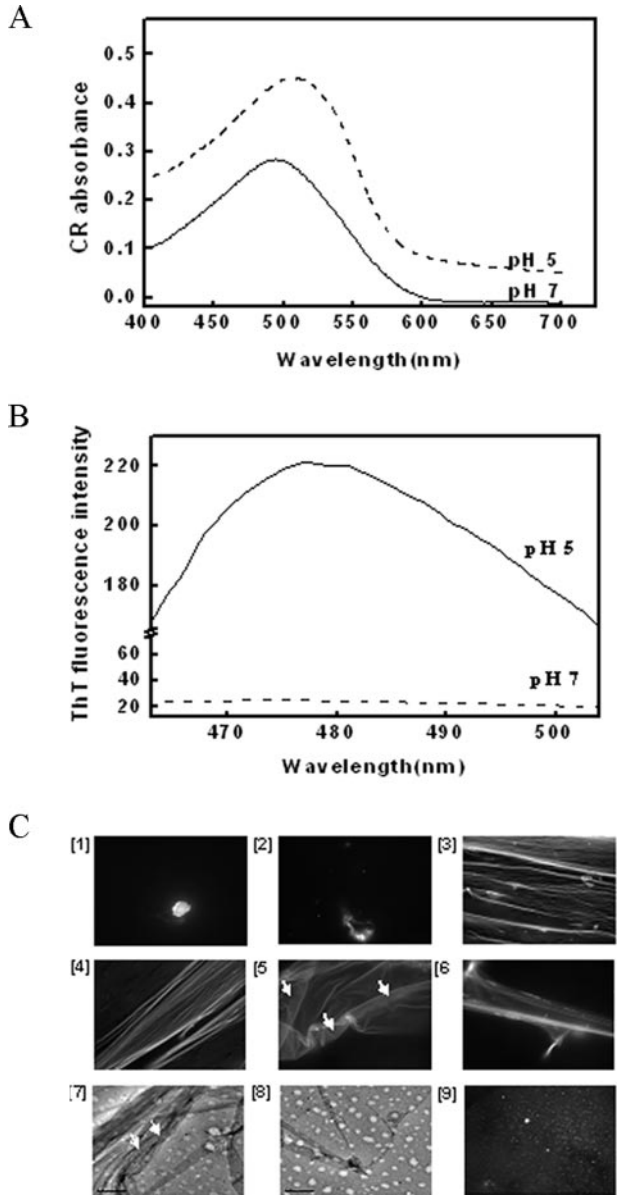

FIGURE 3. **Fibrillation in HylP2.** *A,* binding of Congo red to HylP2. A red shift of ~10 nm in the absorption maximum of the dye was observed with HylP2 at pH 5.0 as compared with HylP2 at pH 7.0. *B,* effect of binding of ThT to HylP2 on the fluorescence spectra of the dye. An enhancement (10-fold) in fluorescence intensity was observed for HylP2 at pH 5.0 as compared with the protein at pH 7.0. *C,* fluorescence and electron micrographs of HylP2. *Panel 1,* fluorescence micrograph of HylP2 during dialysis at pH 5.0, 0 h; *panel 2,* 3 h, both images show no fluorescence and hence no fibrillar structure; *panel 3* 6 h; *panel 4,* 10 h, the image shows parallel arrangement of filamentous structures that do not appear as individual fibers; *panel 5,* 12 h; and *panel 6,* 16 h, total internal reflection fluorescence micrograph showing the presence of a thin film of HylP2. *Arrows* show the folds in this film. *Panels 7* and *8*, electron micrograph of HylP2 at pH 5.0 showing sheet like morphology; *panel 9*, HylP2 at pH 7.0.

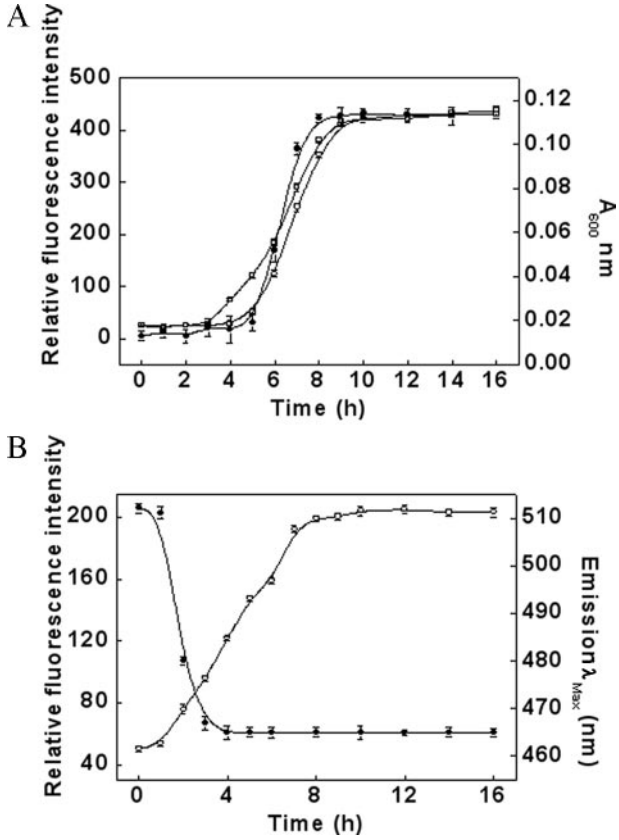

FIGURE 4. **Kinetics of ThT and ANS binding during fibril formation in HylP2.** *A,* kinetics of fibrillation pathway for HylP2 as monitored by changes in ThT fluorescence intensity (○) and light scattering at 600 nm (●) with time. Changes in ThT fluorescence intensity (□) of HylP2 seeded with HylP2 fibrils are shown. *Error bars* indicate the means ± S.E. for all values of ThT binding evident from triplicate measurements. *B,* characterization of protein intermediate involved in fibrillation by ANS fluorescence. Changes in the ANS fluorescence intensity at 465 nm (○) and in the wavelength emission maxima of ANS (●) with time. *Error bars* indicate the means ± S.E. for all values of ANS binding evident from triplicate measurements.

microscopy (Fig. 3*C*). The fluorescence micrographs of HylP2 showed elongated and unbranched filamentous structure placed symmetrically like veins of a leaf. The fibers were then seen to self-assemble into ordered arrays and form a membrane or film in a fluorescence micrograph. Time-dependent analysis of the dialyzed samples of HylP2 at pH 5.0 showed that samples collected in the lag phase of fibril formation showed no ThT binding in fluorescence micrographs, whereas the log phase was marked with the appearance of symmetrically and parallel placed fibers of HylP2. The fluorescence micrographs of HylP2 at the end of log phase demonstrated a thin crumbled membrane-like appearance. The negatively stained electron microscope images of HylP2 also showed a sheet-like feature under similar conditions, which was similar to a synthetic nanofilm (32) or to thin film formed by proteins like squid reflectin (33) or amelogenin (34). No fibrils were detected in HylP2 samples at pH 7.0.

Kinetics of Fibril Formation in HylP2 Stabilized at pH 5.0

To demonstrate that it is the partially unfolded intermediate of HylP2 stabilized at pH 5.0 that undergoes fibril formation as a function of time, we carried out time-dependent binding studies with ThT and ANS. Changes in the ThT fluorescence emission at 480 nm as a function of time on binding to HylP2 at pH 5.0 is shown in Fig. 4*A*. The increase in ThT fluorescence intensity followed a sigmoidal pattern that can be distinctly described in three regions. The initial region of 4 h showed no change in the fluorescence intensity and signified the nucleation or the lag phase. This was followed by the log phase that corresponded to the elongation of the fibrils as demonstrated by a sharp enhancement (about 400 times) for the next 6 h. The final plateau region of the curve reflected the maturation phase

of HylP2 fibril formation. Formation of HylP2 fibrils seeded with preformed HylP2 fibrils was also analyzed, and it was seen that seeding the fibrillation process decreases the lag phase to 3 h as compared with unseeded fibril formation.

The kinetic profile of ANS binding to HylP2 during dialysis at pH 5.0 is shown in Fig. 4*B*. A blue shift in the emission maxima of ANS fluorescence was seen between 1 and 4 h, which indicated that during this period the protein underwent structural changes causing the appearance of solvent-exposed hydrophobic regions in the protein. The formation of this partially folded intermediate species was saturated after 4 h of dialysis. An enhancement in the ANS fluorescence intensity at 465 nm after 4 h indicated an increase in the population of this partially folded stabilized intermediate of HylP2. The combined result of the sigmoidal enhancement of both ANS and ThT binding curves showed that with the enhancement in the population of a partially folded intermediate of HylP2 stabilized at pH 5, the population of the aggregated species was enhanced. Hence, these results explicitly demonstrated that it was the pH 5.0 stabilized partially unfolded species of HylP2 that seeded the fibrillation process in HylP2.

Characterization of the Core Domain in Fibrillar Form of HylP2

The key questions regarding the analysis of the nucleation center in HylP2 fibrils were as follows. First, is the innate domain organization in native HylP2 also conserved in the fibrillar structure of HylP2? Second, which of the structural domains of the enzyme is the core domain in the fibrillation of HylP2?

Protease Sensitivity of the Fibril

Recently, limited proteolysis has been exploited successfully for a number of amyloidogenic proteins, including Aβ peptide, α-synuclein, Ure2p, and bovine α-lactalbumin to analyze portions of the enzyme structure that are involved in fibril formation (35–37). The rationale behind this approach is that proteolytic cleavage generally occurs at flexible regions of the polypeptide chain devoid of hydrogen-bonded regular secondary structures such as α-helices and β-strands. Because there are about 20 cleavage sites for α-chymotrypsin spread throughout the length of the amino acid sequence of HylP2, we therefore used this serine protease for carrying out the limited proteolysis studies. The fibrils of HylP2 at pH 5.0 and native HylP2 at pH 7.0 were incubated for 2 h at 25 °C with α-chymotrypsin in a protein to protease ratio of 500:1, and the proteolyzed samples were analyzed on a 12% SDS-PAGE as shown in Fig. 5*A*. The fragmentation profiles of fibrils of HylP2 and native HylP2 were similar, and in both cases the protein was proteolyzed into two major protein fragments of 25 and 14 kDa, which corresponded to the C- and N-terminal domains respectively, of the protein as established earlier (20). To examine the minimum core portion of the protein involved in fibrillation, we further performed a cleavage of the fibrillar form of HylP2 as well as the native HylP2 with proteinase K. Proteinase K has been used for a number of other amyloid proteins for carrying out cleavage as it is a nonspecific protease and cleaves a protein at all noncompact flexible regions. We used the same protein and protease concentrations for both HylP2 at pH 7.0 and pH 5.0. On examining the proteolyzed samples on the SDS-PAGE (Fig. 5*B*), it was seen that although the native HylP2 was exhaustively chopped into smaller fragments, the fibril of HylP2 at pH 5.0 was proteolyzed into a lower molecular weight species corresponding to a molecular mass of about 25 kDa. This fragment in the HylP2 fibril was obtained consistently at both low and high protease concentrations suggesting that it was very compact and protease-resistant. We hypothesized that this fragment resistant to proteolysis might correspond to either the N- or the C-terminal portion in the fibrillar form of HylP2. Hence, we carried out N-terminal sequencing of the fragment. The amino acids obtained from sequencing of this fragment corresponded to the amino acids (SSSTGGAVN) from residue 127 of the full-length HylP2. The sequencing reports confirmed that this protease-resistant fragment belonged to the C-terminal domain of HylP2. A further conformation of the aforesaid result came from the Western blot analysis of the fragment obtained on proteolysis. The fragment was found to possess affinity for anti-His antibody on Western blot analysis (Fig. 5*C*), thereby demonstrating that this fragment contains the C-terminal His_6 moieties. Because in the recombinant HylP2 protein the histidine tag was present at the C terminus, this fragment corresponded to the C-terminal portion of the protein. The proteolysis studies demonstrated that the domain organization in HylP2

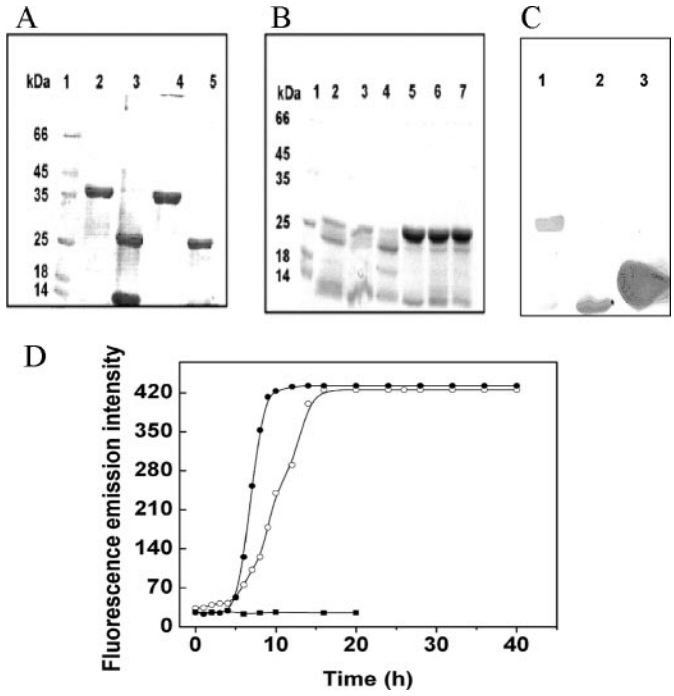

FIGURE 5. **SDS-PAGE profile and Western blot of proteolysis of fibrillar film of HylP2.** *A, lane 1* represents molecular weight markers; *lanes 2* and *4* represent unproteolyzed native and fibrillar form of HylP2, respectively; and *lanes 3* and *5* show the native and the fibrillar forms of HylP2 proteolyzed with α-chymotrypsin, respectively. *B, lane 1* represents molecular weight markers; *lanes 2–4* represent native HylP2 proteolyzed with proteinase K at 1:100 protease to protein concentration. *Lanes 5–7* represent fibrillar of HylP2 proteolyzed with proteinase K at 1:100 at protease to protein ratio for 2, 4, and 6 h, respectively. *C,* Western blot of proteolyzed fragment of fibrillar form of HylP2. *Lanes 2* and *3* represent proteolyzed fragment of fibrillar form of HylP2 with α-chymotrypsin and proteinase K, respectively. *Lane 1* represents unproteolyzed HylP2 as positive control. *D,* kinetics of fibrillation pathway for HylP2 as monitored by changes in ThT fluorescence intensity. ●, full-length HylP2; ○, N- + C-terminal domains (N·C complex) of HylP2; and ■ C-terminal domain of HylP2 at pH 5.0.

remained intact during structural transition from native to fibrillar form of HylP2, and the C-terminal domain was the core domain of the fibrillar structure of HylP2. With the aim to identify that whether the removal of the N-terminal domain leads to a disintegration/destabilization of the fibrillar structure of the protein, we carried out ThT binding and analysis of the film-like structure through fluorescence electron microscopy of the residual protease-resistant fragment. Fluorescence emission intensity centered at 480 nm was similar to that observed for the unproteolyzed fibrillar form of HylP2 at pH 5.0, and the digested fibrils when analyzed by fluorescence electron microscopy showed morphology quite similar to that of the undigested fibrils (data not shown). Hence, this indicates that the N-terminal domain is required for the acquisition of the fibril state by the protein, and once acquired the fibrillar structure does not disintegrate even after the removal of the N-terminal domain from HylP2.

N-terminal Domain of HylP2 Modulates the Kinetics of Fibrillation

As reported earlier, limited proteolysis of the native, fully folded HylP2 with α-chymotrypsin in a protein to protease ratio of 100:1 yielded the C-terminal domain (20). The C-terminal domain was purified by affinity chromatography using a nickel-nitrilotriacetic acid column. We conducted time-dependent ThT binding to the isolated C-terminal domain and assessed its propensity to form amyloid fibrils under these conditions. For this the purified C-terminal domain was also dialyzed against the buffer promoting fibril formation of the native HylP2. Despite using a similar concentration of the C-terminal domain as the native protein, fibril formation was not observed under conditions used for fibrillation of native HylP2 (Fig. 5*D*). Fibril formation was also followed using both the N- and C-terminal domains present together after proteolysis of the full-length protein. The N-terminal domain of HylP2 is known to hydrophobically cling to the C-terminal domain when present together forming the N·C complex of HylP2 (20). The kinetics of fibrillation of the N·C complex of HylP2 was analyzed by ThT fluorescence as shown in Fig. 5*D*. A sigmoidal curve was obtained for ThT binding to N·C complex of HylP2, which was similar to that obtained with full-length protein at pH 5.0. As demonstrated, the difference in the two kinetic graphs lies in presence of a longer lag phase (8 h) in the N·C complex of HylP2 as compared with full-length HylP2 at pH 5.0. This demonstrated that the N-terminal domain of HylP2 was essential for both the formation as well as the acceleration of fibrillation of HylP2.

Enzymatic Activity of the Fibrillar Film of HylP2

Enzymatic activity is the unquestionable signature for a protein having defined natively folded structure. Formation of fibrils in HylP2 was not accompanied by major changes in the native domain organization and conformation. Hence, we explored the presence of enzymatic activity in the pre-fibrillar intermediate and the mature fibrils of HylP2. Activity was examined with the specific substrate hyaluronic acid and the nonspecific substrate chondroitin sulfate for HylP2 (Fig. 6*A*). After 1 h, at the end of lag (4 h) and log (15 h) phases of ThT binding curves, the protein was found to possess 75, 73, and 68% enzymatic activity, respectively, with hyaluronic acid as compared with that observed for HylP2 at pH 7.0, 0 h (100% enzymatic activity of native protein). The observed minimal decrease in the enzymatic activity with transformation of native HylP2 into its fibrillar form was in accordance to the minimal perturbations observed (at N terminus) in its native configuration. Enzymatic activity observed in the fibril form of HylP2 obtained at the end of the exponential decay in the ThT binding curves was about 20% with chondroitin sulfate as its substrate with maximum activity obtained at low substrate concentration (0.02 mg/ml with chondroitin sulfate, Fig. 6*C*) as compared with native HylP2 at pH 7.0 (0.3 mg/ml). Fibrillar form of HylP2 was found to show high substrate inhibition with saturating concentration of substrate as 0.15 mg/ml of hyaluronic acid (Fig. 6*B*). Previous studies have shown that isolated C-terminal domain of the protein showed activity with both hyaluronic acid and chondroitin sulfate (20), and similar observations were made with the fibrillar structure. Similar to the isolated C-terminal domain, the fibrillar form of HylP2 was also observed to follow the property of "high substrate inhibition" for both HA and CS (Fig. 6, *B* and *C*). The commonality of this property supported the fact that the C-terminal domain was the integral part of the fibrillar film, whereas the N-terminal domain was unfolded forming a quasi-native form of HylP2 that led the fibrillation process. There can be two conceivable reasons for the activity in the fibrillar form of HylP2. First, whether the activity measured for the dialyzed protein solution was accounted for mainly by the aggregated species or a fraction of soluble protein that might possibly have been present in the assay mixture. To rule out the presence of leftover soluble protein in the samples, the dialyzed solution of HylP2 at pH 5.0 was then ultracentrifuged, and activity was measured only in the redissolved pellet. Second, if the fibrillar form of HylP2 is prone to breaking/disintegration on redissolving, it can cause a decrease in enzymatic activity of the protein in fibrillar form as compared with native HylP2. To rule out this possibility, the redissolved samples were checked by ThT binding and fluorescence micrographs. Indeed, the ThT binding property and morphology of amyloid fibrils of HylP2 before and after redissolving were similar, pointing toward the fact that once formed these fibrils are not prone to breaking (Fig. 6*D*). Kinetics of substrate degradation was then performed on the redissolved pellet, and the presence of activity in the sample showed that the fibrillar form of HylP2 contained native-like functional units. The residual activity in amyloid form of HylP2 followed a similar substrate degradation pattern (Fig. 6, *B* and *C*) as that of the isolated C-terminal domain of HylP2 (20).

The structural changes in HylP2 as a function of pH lead to the formation of an enzymatically active fibrillar film, which has been schematically illustrated in Fig. 7. This study strengthened the view that formation of mature fibrils is not always accompanied by loss of biological function in proteins, instead changes in the enzymatic activity depend on the extent of changes in the native structure of the fibril-forming protein.

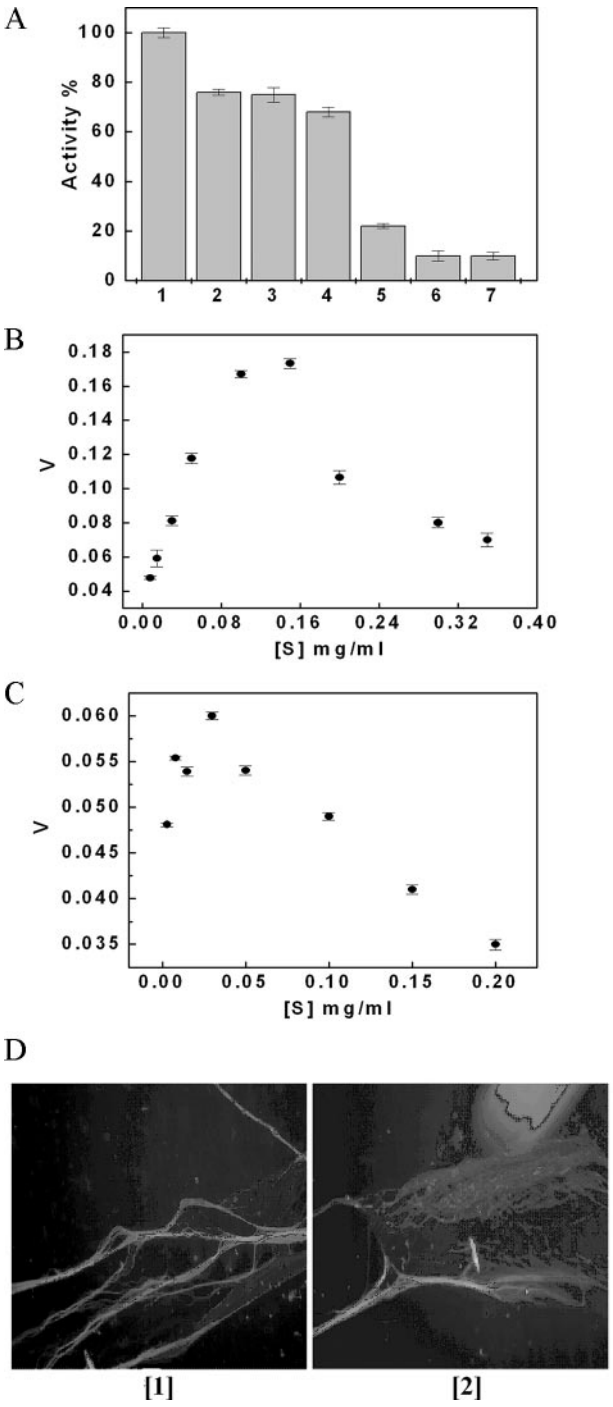

FIGURE 6. **Enzymatic activity profile of native and fibril forms of HylP2.** *A,* activity in native and fibrillar film of HylP2 with HA and CS as substrate for the enzyme. Percentage activity of full-length native HylP2 at pH 7.0 with hyaluronan as its substrate is considered to be 100%. The *bars* indicate the following: *bar 1*, HylP2 at pH 7.0; *bar 2*, HylP2 at pH 5.0 (1 h); *bar 3*, HylP2 at pH 5.0 after 4 h; *bar 4*, fibrillar form of HylP2 at pH 5.0; *bar 5*, after 16 h. Percentage activity of full-length HylP2 in its fibrillar film state at pH 5.0 after 14 h with chondroitin sulfate as substrate. *Bars 6* and *7* represent percentage activity of isolated C-terminal domain of HylP2 at pH 7.0 with hyaluronic acid and chondroitin sulfate, respectively. Residual activity is 11%, which is similar to residual percent activity in the mature fibrillar film form of HylP2 at pH 5.0 for chondroitin sulfate. *Error bars* represent means ± S.E. averaged from velocity measurements taken at saturating substrate concentrations with triplicate samples. *B* and *C,* data points represent "High substrate inhibition" pattern of substrate degradation followed by fibrillar film of HylP2 for hyaluronan and chondroitin sulfate, respectively. The *error bars* represent ± % error obtained in absorbance values at 232 nm obtained from triplicate samples. *D,* fluorescence micrographs of HylP2. *Panel 1*, HylP2 at 1 mg/ml concentration after 14 h of dialysis into CGH buffer at pH 5.0. The micrograph represents a film or ribbon-like morphology on staining with ThT. *Panel 2*, HylP2 at 1 mg/ml and dialyzed for over 14 h was then ultracentrifuged at 80,000 rpm for 2 h. A glossy pellet was obtained and redissolved in CGH buffer (pH 5.0). Fluorescence microscope images were analyzed by methods described under "Fluorescence Microscopy." The images resembled each other in the presence of a similar film-like morphological structure of HylP2. Hence, redissolving did not break the fibrillar film of HylP2.

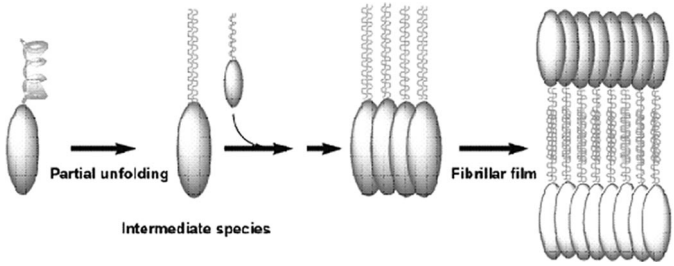

FIGURE 7. **Schematic representation of the fibrillation pathway in HylP2.** The scheme shows that lowering the pH of HylP2 from 7.0 to 5.0 leads to partial unfolding of the N-terminal domain while the trimeric C-terminal domain remains unaltered. Formation of this intermediate species is the critical event leading to formation of higher order aggregates of HylP2. The partially unfolded HylP2 molecules then associate together to form high molecular weight aggregates, which show dye binding properties and ANS binding properties. These filamentous/fibrillar units later collapse into an ordered array and appear as a thin film.

Conclusion

The results outlined above demonstrated that the full-length HylP2 and the N- + C-terminal domain of HylP2 can form fibrils *in vitro* over a pH range of 3.0–5.0 on a time scale commensurate with biophysical measurements. Limited proteolysis revealed that the domain organization is conserved in HylP2 even after the structural transition because of change in pH, and that the N-terminal domain affects the rate of fibril formation. Once formed, complete cleavage and removal of the N-terminal domain do not destabilize the fibrillar structure. The N- and C-terminal domains present together form fibrils but with delayed kinetics as compared with the native unproteolyzed HylP2, whereas the C-terminal domain alone cannot aggregate into fibrillar structures. The limited proteolysis data allowed us to speculate that the C-terminal domain is the minimal compact structure of the fibril of HylP2 protein and was not found to be digested even after prolonged digestion with the protease. This result is in accord with the finding that fibrils are usually resistant to proteolysis (38–41) and structurally consist of several twisted filamentous units of protein (41, 42). Hence, the protein molecules lying within the twisted morphology of these proto-filaments are not accessible to any protease, as the C-terminal domain of HylP2 in this case. The C-terminal domain does not contain the fibrillar core, as the isolated C-terminal domain is not seen to form amyloid film under similar experimental conditions as the full-length protein. But the active site of HylP2 lies at the C-terminal domain (20). Despite the fact that the active site is located at the C-terminal domain of HylP2, it shows 70% activity with its substrate hyaluronic acid, which can be due to the unfolding of the N-terminal domain of HylP2 during the formation of fibrillar film (Fig. 7). It also suggests that the entire sequence of the protein molecule is not incorpo-

rated in the fibrillar core structure and is well supported by earlier studies made on Tau protein and α-synuclein (35, 43).

To date, fibril formation has not been studied in the hyaluronidase family of proteins. The conclusion that fibril formation in the bacteriophage hyaluronidase occurs as a function of pH and begins at a pH value of 5.0, which is very close to the pH of maximal activity of the protein (pH 6.2), is interesting because such a phenomenon *in vivo* could be expected to occur during the intermediacy of the phage hyaluronate lyase with the acidic extracellular bacterial matrix. Bacteriophage is a prominent source of transferring virulent genes to bacteria; hence, functionality in HylP2 over a wide range of pH and resistance to pH appears to be essential for phage infection. Because chondroitin sulfate is present only in mammalian connective tissues, the acquisition of enzymatic activity toward chondroitin sulfate by HylP2 also suggests that the enzyme of this temperate bacteriophage might assist in the bacterial invasion of host tissue, and therefore it serves as an adaptation for the bacterium as well as for the phage. Thus, our investigation illustrates the diversity of fibrillar function across genomes and demands the need to study its occurrence.

Acknowledgments—We thank Dr. C. M. Gupta for constant support provided during the studies. We also thank Dr. W. L. Hynes for providing the plasmid pSF49 used in the study.

REFERENCES

1. Wetzel, R. (1996) *Cell* **6,** 699–702
2. Sunde, M., and Blake, C. C. F. (1998) *Quart. Rev. Biophys.* **31,** 1–39
3. Sunde, M., and Blake, C. C. F. (1997) *Adv. Protein Chem.* **50,** 123–159
4. Dobson, C. M. (2003) *Nature* **426,** 884–890
5. Chiti, F., Taddei, N., Bucciantini, M., White, P., Ramponi, G., and Dobson, C. M. (2000) *EMBO J.* **19,** 1441–1449
6. Kelly, J. W. (1998) *Curr. Opin. Struct. Biol.* **8,** 101–106
7. Dumoulin, M., Canet, D., Last, A. M., Pardon, E., Archer, D. B., Muyldermans, S., Wyns, L., Matagne, A., Robinson, C. V., Redfield, C., and Dobson, C. M. (2005) *J. Mol. Biol.* **346,** 773–788
8. Guijarro, J. I., Sunde, M., Jones, J. A., Campbell, I. D., and Dobson, C. M. (1998) *Proc. Natl. Acad. Sci. U. S. A.* **95,** 4224–4228
9. Uversky, V. N., and Fink, A. L. (2004) *Biochim. Biophys. Acta* **1698,** 131–153
10. Jahn, T. R., and Radford, S. E. (2008) *Arch. Biochem. Biophys.* **469,** 100–117
11. Dobson, C. M. (1999) *Trends Biochem. Sci.* **24,** 329–332
12. Bieler, S., Estrada, L., Lagos, R., Baeza, M., Castilla, J., and Soto, C. (2005) *J. Biol. Chem.* **280,** 26880–26885
13. Plakoutsi, G., Bemporad, F., Calamai, M., Taddie, N., Dobson, C. M., and Chiti, F. (2005) *J. Mol. Biol.* **351,** 910–922
14. Bucciantini, M., Giannoni, E., Chiti, F., Baroni, F., Formigli, L., Zurdo, J., Taddei, N., Ramponi, G., Dobson, C. M., and Stefani, M. (2002) *Nature* **416,** 507–511
15. Walsh, D. M., Klyubin, I., Fadeeva, J. V., Cullen, W. K., Anwyl, R., Wolfe, M. S., Rowan, M. J., and Selkoe, D. J. (2002) *Nature* **416,** 535–539
16. Bucciantini, M., Calloni, G., Chiti, F., Formigli, L., Nosi, D., Dobson, C. M., and Stefani, M. (2004) *J. Biol. Chem.* **279,** 31374–31382
17. Sambashivan, S., Lui, Y., Sawaya, M. R., and Eisenberg, D. (2005) *Nature* **437,** 266–269
18. Fowler, D. M., Koulov, A. V., Alory-Jost, C., Marks, M. S., Balch, W. E., and Kelly, J. W. (2006) *PLoS Biol.* **4,** e6
19. Maxted, W. R. (1952) *Nature* **170,** 1020–1021
20. Mishra, P., Akhtar, S., and Bhakuni, V. (2006) *J. Biol. Chem.* **281,** 7143–7150
21. Gebbink, M. F., Claessen, D., Bouma, B., Dijkhuizen, L., and Wösten, H. A. (2005) *Nat. Rev. Microbiol.* **3,** 333–341
22. Pritchard, D. G., Lin, B., Willingham, T. R., and Baker, J. R. (1994) *Arch. Biochem. Biophys.* **315,** 431–437
23. Naiki, H., Higuchi, K., Hosokawa, M., and Takeda, T. (1989) *Anal. Biochem.* **177,** 244–249
24. Glenner, G. G., Eanes, E. D., and Page, D. L. (1972) *J. Histochem. Cytochem.* **20,** 821–826
25. Tan, Y. J., Oliveberg, M., Davis, B., and Fresht, A. R. (1995) *J. Mol. Biol.* **254,** 980–992
26. Lackowicz, J. R. (1983) *Principles of Fluorescence Spectroscopy*, Plenum Publishing Corp., New York
27. Fink, A. L. (1999) in *Protein: Structures and Molecular Properties* (Creighton, T. E., ed) pp. 140–142, John Wiley & Sons, Inc., New York
28. Semisotnov, G. V., Rodionova, N. A., Razgulyaev, O. I., Uversky, V. N., Gripas', A. F., and Gilmanshin, R. I. (1991) *Biopolymers* **31,** 119–128
29. Stryer, L. (1965) *J. Mol. Biol.* **13,** 482–495
30. Inouye, H., and Kirschner, D. A. (2000) *J. Struct. Biol.* **130,** 123–129
31. LeVine, H., III (1993) *Protein Sci.* **2,** 404–410
32. Marris, E. (2006) *Nature* **444,** 985–991
33. Kramer, M. R., Crookes-Goodson, J. W., and Naik, R. (2006) *Nature* **6,** 533–538
34. Du, C., Falini, G., Fermani, S., Abbot, C., and Moradian-Oldak, J. (2005) *Science* **307,** 1450–1454
35. Miake, H., Mizusawa, H., Iwatsubo, T., and Hasegawa, M. (2002) *J. Biol. Chem.* **277,** 19213–19219
36. Thual, C., Komar, A. A., Bousset, L., Fernandez-Bellot, E., Cullin, C., and Melki, R. (1999) *J. Biol. Chem.* **274,** 13666–13674
37. de Laureto, P. P., Frare, E., Battaglia, F., Mossuto, M. F., Uversky, V. N., and Fontana, A. (2005) *FEBS J.* **272,** 2176–2188
38. Zurdo, J., Guijarro, J. I., and Dobson, C. M. (2001) *J. Am. Chem. Soc.* **123,** 8141–8142
39. Polverino de Laureto, P., Taddei, N., Frare, E., Capanni, C., Costantini, S., Zurdo, J., Chiti, F., Dobson, C. M., and Fontana, A. (2003) *J. Mol. Biol.* **334,** 129–141
40. Fink, A. L. (1998) *Folding Des.* **3,** R9–R23
41. Serpell, L. C. (2000) *Biochim. Biophys. Acta* **1502,** 16–30
42. Jimenez, J. L., Tennent, G., Pepys, M., and Saibil, H. R. (2001) *J. Mol. Biol.* **311,** 241–247
43. Von Bergen, M., Barghorn, S., Muller, S. A., Rickardt, M., Biernat, J., Mandelkow, E. M. Davies, P., Aebi, U., and Mandelkow, E. (2006) *Biochemistry* **45,** 6446–6457
44. Smith, N. L., Taylor, E. J., Lindsay, A., Charnock, S. J., Turkenburg, J. P., Dodson, E. J., Davies, G. J., and Black, G. (2005) *Proc. Natl. Acad. Sci. U. S. A.* **102,** 17652–17657